[4] J. M. Paillot, J. C. Nallatamby, M. Hessane, R. Quere, M. Prigent, and J. Rousset, "A general program for steady state and FM noise analysis of microwave oscillators," in *IEEE MTT-S Int. Microwave Symp. Dig.*, Dallas, TX, 1990, pp. 287–1290.
[5] R. Adler, "A study of locking phenomena in oscillators," *Proc. IRE*, vol. 34, pp. 351–357, June 1946.
[6] A. Blanchard, *Technique des boucles d'asservissement de phase*. Paris, France: Cours de l'École Supérieure d'Électricité, Univ. Paris, 1975.

Static Analysis of Arbitrarily Shaped Conducting and Dielectric Structures

Sadasiva M. Rao and Tapan K. Sarkar

***Abstract*—In this paper, a simple and efficient numerical procedure is presented to compute the charge distribution and capacitance of conducting bodies in the presence of dielectric structures of arbitrary shape and finite size. The method presented is robust and provides accurate results for both low as well as high dielectric-constant materials as supported by numerical examples.**

***Index Terms*—Capacitance, dielectric bodies, electrostatic analysis, moment methods.**

I. Introduction

In [1], Rao *et al.* described the evaluation of static charge distribution and capacitance matrices for conductors of finite size in the presence of dielectric media. Recently, this formulation was also incorporated into a fast multipole method to generate a computationally fast algorithm [2], [3]. Although the work presented in [1] and [2] is general, it is computationally expensive. In [1], the total charge is computed everywhere by solving a set of integral equations, the free charge on conductors is then obtained by solving yet another integral equation. Thus, the free-charge extraction is a two-step procedure and, computationally, this implies storing and inverting large matrices. Further, the method presented in [1] may be inaccurate, as shown in [3], for the case of high-dielectric materials.

In this paper, we present a simple and efficient procedure to obtain the free charge on the conductors in the presence of dielectric materials which may have low as well as large ϵ_r. The main advantage of this technique is the elimination of the expensive two-step procedure and calculating the free charge in a straightforward manner.

II. Integral-Equation Formulation

Consider a system of finite length, and finite- or zero-thickness conductors situated in the presence of dielectric bodies, as shown in Fig. 1. Let N_c and N_d represent the total number of disjoint conductors and dielectric bodies, respectively, which are present in the system configuration. The whole system is immersed in free space and could be placed on a ground plane of either finite or infinite size.

Manuscript received April 24, 1997; revised May 11, 1998.
S. M. Rao is with the Department of Electrical Engineering, Auburn University, Auburn, AL 36849 USA.
T. K. Sarkar is with the Department of Electrical Engineering and Computer Science, Syracuse University, Syracuse, NY 13244 USA.
Publisher Item Identifier S 0018-9480(98)05500-8.

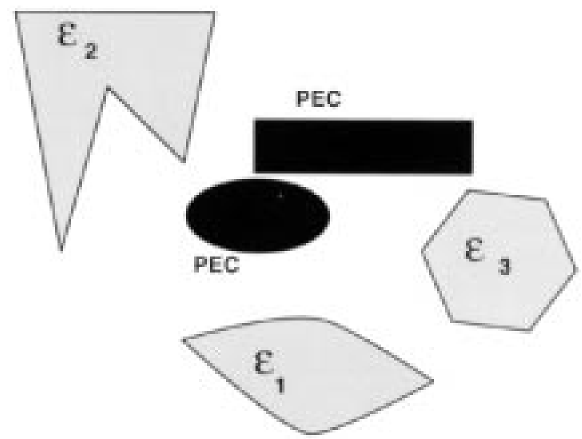

Fig. 1. Conducting and dielectric structures in the homogeneous medium.

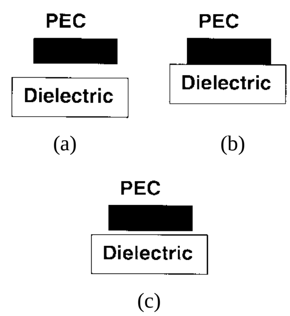

Fig. 2. Numerical modeling procedure.

In this formulation, the central idea is that we treat each conductor and each dielectric body as if it is immersed in free space. Thus, we consider a combination of the conductor–dielectric interface as two bodies separated by zero distance. In this way, we treat all dielectric bodies as closed surfaces. If the conducting and dielectric bodies are separated by a finite distance, as shown in Fig. 2(a), the treatment is obvious. However, if the conductor and dielectric bodies are joined together, as shown in Fig. 2(b), we treat them as two bodies with a layer of zero-thickness free space separating them, as shown in Fig. 2(c).

In applying the equivalent charge formulation, we first replace each conducting and dielectric surface by surface charges σ_c and σ_d, respectively. Using the mathematical procedures described in [1], we derive a set of integral equations, given by

$$\sum_{i=1}^{N_c+N_d} \frac{1}{4\pi\epsilon_0} \int_{S_i} \frac{\sigma(\boldsymbol{r}')}{|\boldsymbol{r}-\boldsymbol{r}'|}\, ds' = V_j(\boldsymbol{r}), \qquad \boldsymbol{r} \in S_j,\ j = 1, 2, \cdots, N_c \tag{1}$$

and

$$2\pi(1+\epsilon_{rj})\sigma(\boldsymbol{r})+(1-\epsilon_{rj}) \sum_{i=1}^{N_c+N_d} \int_{S_i} \frac{\sigma(\boldsymbol{r}')(\boldsymbol{r}-\boldsymbol{r}')\cdot \boldsymbol{a}_{nj}}{|\boldsymbol{r}-\boldsymbol{r}'|^3}\, ds' = 0, \qquad \boldsymbol{r} \in S_j,\ j = N_c+1, N_c+2, \cdots, N_c+N_d \tag{2}$$

where V_j is the potential on the jth conductor, ϵ_{rj} and $\boldsymbol{a}_{nj}$ are the dielectric constant and unit outward normal of the jth dielectric body, and σ is the unknown charge density equal to σ_c or σ_d. Note that $\boldsymbol{a}_{nj}$ may be uniquely defined since the dielectric body is a closed body.

Thus, it is quite clear that by solving (1) and (2), we obtain the free charge on the conductor without any further processing. Also, in (1) and (2), $\boldsymbol{r}$ and $\boldsymbol{r}'$ represent the position vectors to observation and source points with respect to a global coordinate origin, respectively.

III. Numerical Solution

In order to determine σ numerically, the surface of each conducting and dielectric body is discretized into a set of triangular patches and the charge density is assumed to be constant over a given patch. Thus, dividing the ith surface into N_i patches, we have

$$N = \sum_{i}^{N_c} N_i + \sum_{i}^{N_d} N_i = N_a + N_b \tag{3}$$

where N, N_a, and N_b represent the total number of triangles in the geometrical model, number of patches on the conductors, and number of patches on the dielectric bodies, respectively.

For the method-of-moments solution [4], we select the basis as well as the testing functions as

$$f_p(\boldsymbol{r}) = \begin{cases} 1.0, & \boldsymbol{r} \in T_p \\ 0.0, & \text{otherwise} \end{cases} \tag{4}$$

where T_p is the pth triangular patch in the grid scheme.

First, we consider the testing procedure. Defining the inner product as

$$\langle f, g \rangle = \int_s f g \, ds \tag{5}$$

we have

$$\left\langle f_p, \sum_{i=1}^{N_c+N_d} \frac{1}{4\pi\epsilon_0} \int_{S_i} \frac{\sigma(\boldsymbol{r}')}{|\boldsymbol{r}-\boldsymbol{r}'|} ds' \right\rangle = \langle f_p, V_j(\boldsymbol{r}) \rangle \tag{6}$$

for $p = 1, 2, \cdots, N_a$, and

$$\langle f_p, 2\pi(1+\epsilon_{rj})\sigma(\boldsymbol{r}) \rangle + \left\langle f_p, (1-\epsilon_{rj}) \sum_{i=1}^{N_c+N_d} \int_{S_i} \frac{\sigma(\boldsymbol{r}')(\boldsymbol{r}-\boldsymbol{r}')\cdot \boldsymbol{a}_{nj}}{|\boldsymbol{r}-\boldsymbol{r}'|^3} ds' \right\rangle = 0 \tag{7}$$

for $p = N_a + 1, \cdots, N$.

Using (4) as expansion functions, we then approximate the charge density σ as

$$\sigma(\boldsymbol{r}) = \sum_{q=1}^{N} \sigma_q f_q \tag{8}$$

where σ_q are the unknown coefficients to be determined.

Substituting (8) in (6) and (7), we obtain a matrix equation given by

$$[\boldsymbol{Z}][\boldsymbol{Q}] = [\boldsymbol{V}] \tag{9}$$

where the matrix element Z_{pq} is given by

$$z_{pq} = \begin{cases} \dfrac{1}{4\pi\epsilon_0} \displaystyle\int_{T_p}\int_{T_q} \frac{ds'\,ds}{|\boldsymbol{r}-\boldsymbol{r}'|}, & \text{for } p = 1, 2, \cdots, N_a; \; q = 1, 2, \cdots, N \\ 2\pi(1+\epsilon_{rp})A_p, & \text{for } p = q;\; p, q > N_a \\ (1-\epsilon_{rp}) \displaystyle\int_{T_p}\int_{T_q} \frac{(\boldsymbol{r}-\boldsymbol{r}')\cdot \boldsymbol{a}_{np}}{|\boldsymbol{r}-\boldsymbol{r}'|^3} ds'\,ds, & \text{for } p \neq q;\; p > N_a; \; q = 1, 2, \cdots, N. \end{cases} \tag{10}$$

Also, the matrix elements for the excitation vector are given by $V_p A_p$ for $p < N_a$ and zero, otherwise.

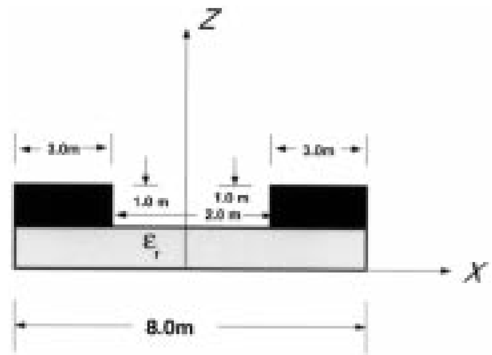

Fig. 3. Two conducting cylinders of rectangular cross section (3.0 m × 1.0 m) mounted over a dielectric bed situated on a ground plane. The length of the structure in y-dimension is 10 m.

TABLE I
Capacitance Matrix for the Two-Conductor System (Capacitance in Nano-Farads)

$\epsilon_r = 1.0$		$\epsilon_r = 10.0$		$\epsilon_r = 80.0$	
1.2900	-0.0750	3.3825	-0.0777	24.2206	-0.1399
-0.0750	1.2900	-0.0777	3.3825	-0.1406	24.2208

In (10), ϵ_{rp}, $\boldsymbol{a}_{np}$, and A_p represent the dielectric constant, outward unit normal vector, and area of the pth patch, respectively. The integrations in (10) are performed using analytical and numerical techniques [5].

A close look at (10) indicates that there exists a singularity for $\boldsymbol{r} = \boldsymbol{r}'$ for the patches T_p, T_q, and $p \neq q$. This occurs whenever there is physical contact between two dielectrics or between a dielectric-conducting structures. Evaluating the singular integral using standard mathematics, we get

$$z_{pq} = -2\pi\alpha(1-\epsilon_{rp})A_p \tag{11}$$

where

$$\alpha = \begin{cases} 2\pi, & \text{if } \boldsymbol{r} \text{ is interior to } T_p \\ \pi, & \text{if } \boldsymbol{r} \text{ is on the contour of } T_p \\ \alpha_i, & \text{if } \boldsymbol{r} \text{ is on the } i\text{th vertex of } T_p \end{cases} \tag{12}$$

and α_i is the interior angle of the ith vertex of the triangle T_p.

The superior nature of this method over the previous methods is evident from the simplified mathematical expressions and efficient numerical evaluation. The direct computation of the free-charge density is a major advantage of this approach. This procedure effectively eliminates the storage of two large $N \times N$ matrices.

IV. Numerical Results

In this section, for the sake of conciseness, we present only two numerical examples. However, it may be noted that the method was tested against several published results and found to be accurate in each case.

For the first example, as shown in Fig. 3, each conducting cylinder and dielectric bed was approximated by 172 and 392 triangular patches, respectively, covering all faces. The total number of unknowns in the system is 736. In Table I, we present the capacitance obtained for various permittivity ratios. It may be noted that the capacitance matrix remains symmetric for all cases, thus illustrating the robustness of this formulation.

In the second example, referring to Fig. 4, we have two conducting strips sandwiched between two dielectric beds. Further, two more conductors are located on the second dielectric bed. For this case, the

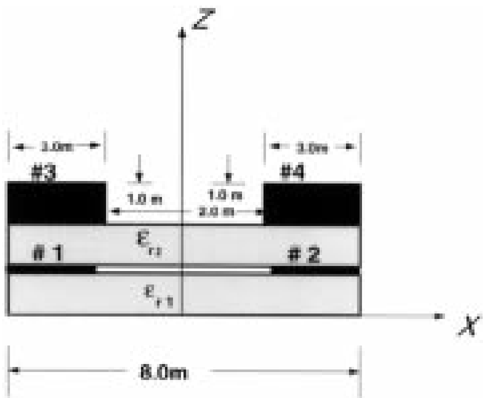

Fig. 4. Two conducting strips (3.0-m width) and two conducting cylinders of rectangular cross section (3.0 m × 1.0 m) mounted over two dielectric beds. The whole structure is situated on a ground plane. The length of the structure in y-dimension is 10 m.

TABLE II
CAPACITANCE MATRIX FOR THE FOUR-CONDUCTOR SYSTEM (CAPACITANCE IN NANO-FARADS)

$\epsilon_{r1} = 1.0$, $\epsilon_{r2} = 1.0$				$\epsilon_{r1} = 60.0$, $\epsilon_{r2} = 30.0$			
0.67	-0.01	-0.29	-0.01	27.33	-0.27	-8.13	-0.16
-0.01	0.67	-0.01	-0.29	-0.27	27.33	-0.16	-8.13
-0.29	-0.01	0.64	-0.09	-8.50	-0.13	9.23	-1.46
-0.01	-0.29	-0.09	0.64	-0.13	-8.50	-1.46	9.23

strips are modeled with 60 triangular patches each. The conducting cylinders and dielectric beds are modeled in the same way as in the previous example. The total number of unknowns for this case is 1248. In Table II, we present the capacitance matrix for two dielectric ratios, which again, remains symmetric.

V. CONCLUSIONS

In this paper, we present a superior method to calculate the charge distribution and capacitance for a system of finite-sized conductors in the presence of arbitrarily shaped dielectric bodies of low, as well as high, dielectric materials.

REFERENCES

[1] S. M. Rao, T. K. Sarkar, and R. F. Harrington, "The electrostatic field of conducting bodies in multiple dielectric media," *IEEE Trans. Microwave Theory Tech.*, vol. MTT-32, pp. 1441–1448, Nov. 1984.
[2] K. Nabors and J. White, "Fastcap: A multipole accelerated 3-D capacitance extraction," *IEEE Trans. Computer-Aided Design*, vol. 11, pp. 1447–1459, Oct. 1991.
[3] X. Cai, K. Nabors, and J. White, "Efficient Galerkin techniques for multipole-accelerated capacitance extraction of 3-D structures with multiple dielectrics," presented at the Proc. Conf. Advanced Res. VLSI, Chapel Hill, NC, 1995.
[4] R. F. Harrington, *Field Computation by Moment Methods.* New York: Macmillan, 1968.
[5] S. V. Yeshantharao, "EMPACK—A software toolbox of potential integrals for computational electromagnetics," M.S. thesis, Dept. Elect. Eng., Univ. Houston, Houston, TX, 1989.

Analysis of a Slot-Coupled T-Junction Between Circular-to-Rectangular Waveguide

S. B. Sharma, S. B. Chakrabarty, and B. N. Das

***Abstract*— This paper presents a rigorous analysis of a slot-coupled T-junction between a primary circular cylindrical waveguide and rectangular waveguide, forming the coupled T-arm. The analysis is based on moment-method formulation using full-wave basis functions and Galerkin's technique for testing. Expression for the coupling and reflection coefficients are found, taking into account the effect of finite wall thickness of the circular waveguide in which the coupling slot is milled. A comparison between the theoretical and experimental results on coupling and return loss are presented.**

I. INTRODUCTION

In view of their wide application in commercial systems as well as laboratory measurements [1]–[5], investigation into different types of aperture-coupled waveguide junctions has attracted the attention of researchers for a long time. Rigorous analysis on the slot-coupled junction between similar and dissimilar waveguides with collinear [6], [7] and orthogonal axes [8] have been carried out. Formulation has been presented for a T-junction [9] and also cascaded sections of junctions [10], in which the primary guide is a rectangular waveguide and the T-arm is a circular waveguide. It is also of importance to study the electrical characteristics of a T-junction, in which the primary waveguide is a circular cylindrical waveguide and the secondary guide is a rectangular waveguide. This was presumably not attempted because of the complexity in finding the internal dyadic Green's function of the circular cylindrical waveguide.

In this paper, analysis based on moment-method formulation using full-wave basis function and the Galerkin's method for testing is presented for derivation of expression for the electrical characteristics of a T-junction between a circular waveguide as the primary waveguide and T-arm as the rectangular waveguide. The coupling takes place through an axial slot in the wall of circular waveguide and in the transverse cross section of the coupled rectangular waveguide. This analysis takes into account the effect of finite wall thickness by considering the possible forward and backward traveling waves in the stub waveguide representing the coupling slot milled in the wall of the cylindrical waveguide of finite wall thickness [11]. The unknown field distribution in the slot aperture is found by transforming the integral equation derived from the boundary conditions for the tangential components of the magnetic fields into a matrix equation. The elements of the matrices are found considering the effect of all possible higher order modes in circular, rectangular, and stub waveguides. From the elements of the scattering matrix derived in this formulation, coupling and return loss are found. A comparison between the theoretical and experimental results are also presented.

Manuscript received April 24, 1997; revised May 11, 1998.
S. B. Sharma and S. B. Chakrabarty are with the MSAD/MSDG/RSA Group, Space Applications Centre, Indian Space Research Organization, Ahmedabad 380 053, India.
B. N. Das is with the Department of Electronics and Electrical Communication Engineering, Indian Institute of Technology, Kharagpur 721 302, India.
Publisher Item Identifier S 0018-9480(98)05499-4.